Accepted Manuscript

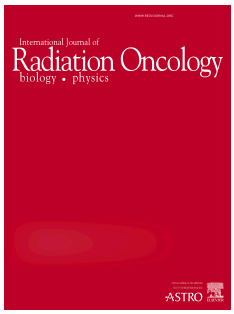

Delineation of neck clinical target volume specific to nasopharyngeal carcinoma based on lymph node distribution and the international consensus guidelines

Li Lin, M.D., Yao Lu, Ph.D., Xiao-Ju Wang, M.D., Hui Chen, B.S., Sha Yu, Ph.D., Jiao Tian, M.S., Guan-Qun Zhou, M.D., Lu-Lu Zhang, M.D., Zhen-Yu Qi, Ph.D., Jiang Hu, M.S., Jun Ma, M.D., Ying Sun, Ph.D.

PII: S0360-3016(17)34083-X

DOI: 10.1016/j.ijrobp.2017.11.004

Reference: ROB 24588

To appear in: *International Journal of Radiation Oncology • Biology • Physics*

Received Date: 19 August 2017

Revised Date: 20 October 2017

Accepted Date: 1 November 2017

Please cite this article as: Lin L, Lu Y, Wang X-J, Chen H, Yu S, Tian J, Zhou G-Q, Zhang L-L, Qi Z-Y, Hu J, Ma J, Sun Y, Delineation of neck clinical target volume specific to nasopharyngeal carcinoma based on lymph node distribution and the international consensus guidelines, *International Journal of Radiation Oncology • Biology • Physics* (2017), doi: 10.1016/j.ijrobp.2017.11.004.

Title page

Delineation of neck clinical target volume specific to nasopharyngeal carcinoma based on lymph node distribution and the international consensus guidelines

Running Title: Delineation of neck CTV specific to NPC

Authors and Affiliations:

Li Lin, M.D.[1*], Yao Lu, Ph.D.[2*], Xiao-Ju Wang, M.D.[1, 3*], Hui Chen, B.S.[2], Sha Yu, Ph.D.[2], Jiao Tian, M.S.[2], Guan-Qun Zhou, M.D.[1], Lu-Lu Zhang, M.D.[1], Zhen-Yu Qi, Ph.D.[1], Jiang Hu, M.S.[1], Jun Ma, M.D.[1], Ying Sun, Ph.D.[1†]

[1] Department of Radiation Oncology, Sun Yat-sen University Cancer Center, State Key Laboratory of Oncology in South China, Collaborative Innovation Center for Cancer Medicine, 651 Dongfeng Road East, Guangzhou 510060, People's Republic of China.

[2] School of Data and Computer Science, Sun Yat-sen University, 132 Waihuan Road East, Guangzhou University City, Guangzhou 510060, People's Republic of China.

[3] Department of Radiation Oncology, Hangzhou Cancer Center, 34 Yan Guan Lane, Zhongshan Road South, Hangzhou 310002, People's Republic of China.

[*] These authors contributed equally to this work.

Correspondence to: Ying Sun

Department of Radiation Oncology, Sun Yat-sen University Cancer Center, State Key Laboratory of Oncology in South China, Collaborative Innovation Center of Cancer Medicine, 651 Dongfeng Road East, Guangzhou 510060, People's Republic of China

Tel.: +86-20-87342253

Fax: +86-20-87343295

E-mail: sunying@sysucc.org.cn

Conflict of Interest Statement

The authors declare no potential conflicts of interest.

Acknowledgments

This work was supported by the grants from Sun Yat-sen University Clinical Research 5010 Program (No.2012011), Health & Medical Collaborative Innovation Project of Guangzhou City, China (No. 201604020003), Special Support Program of Sun Yat-sen University Cancer Center (No. 16zxtzlc06), the Innovation Team Development Plan of the Ministry of Education (No. IR_17R110), the National Natural Science Foundation of China (No. 11401601), and the Science and Technology Innovative Project of Guangdong Province, China (Nos. 2016B030337003).

Delineation of neck clinical target volume specific to nasopharyngeal carcinoma based on lymph node distribution and the international consensus guidelines

Abstract

***Purpose*:** To establish regional lymph node (LN) distribution probability map and draw neck clinical target volume (CTV) specific to nasopharyngeal carcinoma (NPC).

Methods and Materials: One thousand patients with pathologically-proven NPC between January 2010 and December 2011 were enrolled. Center points of LNs with a minimal axial diameter (MID) ≥ 4 mm were marked on one single treatment planning computed tomography scan. Neck node levels I – X based on the 2013 updated international consensus guidelines were also contoured. LN distribution probability maps and distribution curves were established. Relationships between LN distribution and consensus guidelines were analyzed to propose modifications for CTV boundaries specific to NPC.

***Results*:** A total of 10651 LNs from 959 patients were marked. Based on the distribution of LNs and consensus guidelines, the majority of node levels defined in the 2013 updated consensus guidelines were confirmed to be comprehensive and applicable for NPC. However, for level Vb, 13.3% (11/83) cases had LNs beyond the posteromedial border; for level VIIa (retropharyngeal LN), 1.5% (12/819) cases had LNs above the cranial boundary and 5 cases had LNs emerged in the medial group. Moreover, we confirmed that no LN had been detected in certain areas of level Ib, II, IVa and Vc. Accordingly, a new level VIIc was proposed to include medial group of retropharyngeal LNs, and moderate extended boundaries for levels Vb and VIIa were recommended, while reduced boundaries were possibly adaptable for levels Ib, II, IV and Vc.

***Conclusion*:** The majority of node levels in the 2013 updated consensus guidelines are comprehensive

and applicable for NPC. While, we propose a new level VIIc to include medial group of retropharyngeal LNs, recommend moderate extended boundaries for levels Vb and VIIa, and suggested that boundaries for levels Ib, II, IV and Vc might be reduced.

Introduction

Early, widespread neck lymph node (LN) involvement is a well-recognized clinical feature of nasopharyngeal carcinoma (NPC) due to the vast submucosal avalvular lymph capillary network. Retrospective studies showed that up to 40% of node-negative patients staged using palpation subsequently developed lymphadenectasis without elective neck irradiation (1). A meta-analysis reported that 85% of 2920 Chinese NPC patients staged using magnetic resonance (MR) imaging had LN involvement at diagnosis (2). Therefore, elective neck irradiation was a standard recommendation for all patients in the conventional radiotherapy era, and continued in the intensity-modulated radiotherapy (IMRT) era.

The highly conformal dose distribution of IMRT requires precise delineation of the gross tumor volume (GTV) and clinical target volume (CTV). Precise knowledge of normal neck LN anatomy and translation of anatomic boundaries on computed tomography (CT) or MR images is crucial for delineation of the neck CTV during IMRT planning. CT-based international consensus guidelines for delineation of the neck CTV in node-negative patients were proposed in 2003 based on the Robbins Classification by major cooperative groups in Europe and North America (3). The guideline was extended to include the node-positive and post-operative neck in 2006 (4) and updated to include more comprehensive neck node levels with more concise descriptions of anatomic boundaries in 2013 (5).

The guidelines facilitate uniform delineation of neck CTV by radiation oncologists and enables institutions to share data. However, as these guidelines were primarily derived from patients with head and neck squamous cell cancer, whether they are optimal for NPC is unknown. With the aim of providing more suitable boundaries for neck CTV delineation in NPC, we established regional lymph

node distribution probability maps based on a large cohort of patients by marking LNs on one single template CT scan; then compared LN distribution for NPC with the 2013 updated consensus guidelines to draw neck CTV boundaries specific for NPC.

Methods and Materials

Patients

For establishment of regional lymph node distribution probability map, 1000 patients with pathologically-proven, non-disseminated NPC diagnosed between January 2010 and December 2011 were enrolled. Inclusion criteria for eligible patients were: (1) ≥ 18-years-old; (2) underwent baseline MRI scans of nasopharynx and neck, with images stored in our institutional Picture Archiving and Communication System; (3) completed radical IMRT. We excluded patients with (1) history of head and neck surgery; (2) obvious artifacts on MRI images that influenced LN defining; or (3) insufficient MR scanning scope to cover nasopharynx and neck. This study was approved by the Institutional Review Board; requirement to obtain informed consent was waived.

Template CT scan

One patient's treatment planning CT scan with contrast was selected as the template for marking exact position of LNs. Selection criteria were: (1) T1N0 disease without obvious soft tissue masses; (2) no artifacts; (3) patient immobilized in supine and "neutral" position using head, neck and shoulder thermoplastic mask; (4) without obvious bilateral asymmetry in anatomical structure; (5) region from head to 2 cm below sternoclavicular joint included in CT scan; (6) enough fatty space to distinguish anatomy.

The selected CT scan were captured in 3 mm slices from the head to 2 cm below sternoclavicular joint (matrix size, 512×512; voxel resolution, $0.97 \times 0.97 \times 3.0$ mm in left-right, antero-posterior and cranio-caudal directions).

Lymph node marking

Retropharyngeal LNs (LN_{RP}) and cervical LNs displaced on MR image with a minimal axial diameter (MID) ≥ 4 mm were marked on the template CT slice-by-slice. Each eligible LN was manually marked at the equivalent location in template CT with reference to adjacent anatomic landmarks based on pretreatment MR image and original treatment planning CT. Referenced anatomic landmarks mainly included main vessels, bones, muscles and organs described in the 2013 update international consensus guidelines. MR imaging protocol and detailed standard operating procedure of LN marking is described in the supplementary methods. Two independent operators participated: a marker (with 5 years of experience in radiotherapy of NPC) to mark and a reviewer (with more than 15 years of experience in radiotherapy of NPC) to independently check; disagreements were resolved by consensus. Any LN appearing in the medial retropharyngeal group was marked despite of size. Monaco® version 5.0 (Elekta AB, Stockholm, Sweden) was used for LN marking. Circles with a diameter of 3 mm (the smallest circle generated by Monaco) were used to mark the central points of each LN on all emerged slices. Fig. 1 gives visual examples of LN marking on the template CT scan.

Cervical LNs marked on the template CT scan meeting the diagnostic criteria for LN metastases were defined as $LN_{\geq 10mm}$; LNs with a MID of 8 – 10 mm (11 mm for levels Ib and IIa) or 4 – 8 mm without any other positive criteria, as $LN_{8\text{-}10mm}$ and $LN_{4\text{-}8mm}$, respectively. Diagnostic criteria for positive cervical LNs were: (1) any cervical LN with a minimal axial diameter (MID) ≥ 10 mm (level Ib and IIa, ≥ 11 mm); (2) LNs of any size with central necrosis: a focal area of high signal intensity on T2-weighted images or a focal area of low signal intensity on T1-weighted images with or without a contrast-enhanced rim; and (3) LNs of any size with extra-capsular spread: the presence of indistinct LN margins, irregular LN capsular enhancement, or infiltration into the adjacent fat or muscle.

Neck node levels, including levels Ia, Ib, II, III, IVa, IVb, Va, Vb, Vc, VIa, VIb, VIIa, VIIb, VIII, IX, Xa and Xb, was replicated on template CT scan with reference to 2013 updated consensus guidelines by two physicians in collaboration. To avoid potential bias in node levels delineation, marked LNs were blinded.

Data preparation

Template CT scan, marked LNs and contoured neck node levels were exported from Monaco in DICOM-RT format and converted into TXT format using in-house software developed with Matrix Laboratory (MATLAB 2015a, Mathworks, Natick, MA, USA).

Regional lymph node distribution characteristics

To study regional LN distribution, marked cervical LNs were organized in three patterns: (1) $LN_{\geq 10mm}$; (2) $LN_{\geq 8mm}$, combining $LN_{\geq 10mm}$ and $LN_{8\text{-}10mm}$; and (3) $LN_{\geq 4mm}$, combining $LN_{\geq 10mm}$, $LN_{8\text{-}10mm}$ and $LN_{4\text{-}8mm}$. Though center points of each LN on all emerged slices were marked, to minimize mass and distortion effects of enlarged nodes, only center point of the median slice of each LN was used for analysis. LN distribution characteristics were summarized by patients and by nodes. When summarized by patients, the incidence was defined as the ratio of the number of patients presenting with LN at certain level and pattern and total patient number. When calculated by nodes, the incidence was defined as the ratio of the number of LNs at certain level and pattern and the total LN number of that pattern.

Regional lymph node distribution probability map and distribution curves

To generate LN distribution probability map, firstly the template CT was discretized to a

three-dimensional mesh with sphere grids (resolution, 6 mm); then LN numbers within each grid were computed and translated into relative values, which defined as LN number within one grid divided by the maximum LN number within any of the grids. Color change was implemented to demonstrate distinct relative values. Three heat maps were generated: $Map_{\geq 10mm}$, by LN_{RP} and $LN_{\geq 10mm}$; $Map_{\geq 8mm}$, by LN_{RP} and $LN_{\geq 8mm}$; and $Map_{\geq 4mm}$, by LN_{RP} and $LN_{\geq 4mm}$. Corresponding LN distribution curves (named $DC_{\geq 10mm}$, $DC_{\geq 8mm}$, $DC_{\geq 4mm}$) were generated to encircle all LNs in each pattern.

Relationship between distribution curves and 2013 updated consensus guidelines node levels

To draw specific neck CTV for NPC from 2013 updated consensus guidelines, relationship between $DC_{\geq 4mm}$ and consensus node levels was analyzed by two radiation oncologist with more than 15 years of experience in radiotherapy of NPC. Node levels were classified into three categories: (1) levels with no distribution curves being generated; (2) levels with $DC_{\geq 4mm}$ being completely included in the consensus node levels; (3) levels with $DC_{\geq 4mm}$ exceeding the consensus node levels.

Results

Patient and regional lymph node distribution characteristics

Characteristics of the patients and regional lymph nodes distribution are summarized in Table 1 and Table 2 respectively. Of 1000 patients, 959 (95.9%) had LNs with a MID ≥ 4 mm, in which 819 (85.4%) presented with LN_{RP}, 605 (63.1%) with $LN_{\geq 10mm}$, 353 (36.8%) with $LN_{8\text{-}10mm}$, and 945 (98.5%) with $LN_{4\text{-}8mm}$. A total of 10651 LNs were marked: 1625 (15.3%) were LN_{RP} (level VIIa), 2693 (25.3%) were $LN_{\geq 10mm}$, 504 (4.7%) were $LN_{8\text{-}10mm}$ and 5829 (54.7%) were $LN_{4\text{-}8mm}$. In general, incidences of $LN_{\geq 8mm}$ and $LN_{\geq 10mm}$ were similar for all node levels, and when it came to $LN_{\geq 4mm}$, incidences increased sharply, especially levels Ia from 4 (0.08%) to 142 (1.3%) and Ib from 62 (1.3%) to 1084 (10.2%).

Five (0.3%) of 1625 LN_{RP} were located in the medial group. Only two nodes with a MID of 4 – 8 mm were found in level VIb and no LN with a MID of ≥ 4 mm in level VIa. No $LN_{\geq 10mm}$ emerged in levels Ia, VIa, and VIb.

Regional lymph node distribution probability maps

Probability maps ($Map_{\geq 10mm}$, $Map_{\geq 8mm}$ and $Map_{\geq 4mm}$) of neck node distribution are shown in Fig. 2 through 5 typical transverse sections (Fig. E1 – 3 gives the entire maps). Color wash changing from blue through yellow to red indicates probability increase. From probability maps, distinct LN distribution probabilities of different levels are observed, and the detailed location of LNs in each level can be intuitively exhibited. For example, from level II to Level IV, LNs emerged before carotid sheath become fewer.

Regional lymph node distribution curves

Visual examples of distribution curves ($DC_{\geq 10mm}$, $DC_{\geq 8mm}$ and $DC_{\geq 4mm}$) along with 2013 updated consensus guidelines node levels are shown in Fig. 3 through 8 transverse sections (Fig. E4 gives entire distribution curves). Distribution curves for $DC_{\geq 10mm}$ and $DC_{\geq 8mm}$ were nearly the same; when along with $LN_{4\text{-}8mm}$, LNs became more profuse in levels Ia, Ib, IVa, IVb, Vb and Vc, and the distribution curve extended markedly.

According to the relationships between $DC_{\geq 4mm}$ and consensus guidelines node levels, Level VIa had no distribution curve generated, levels Ib, II, III, IVa, IVb, Va, Vc, VIb, VIIa, VIIb, VIII, IX, Xa had distribution curves being completely encompassed by the consensus guidelines node levels, and levels Vb and VIIa had distribution curves exceeding the boundaries defined in the consensus guidelines. More specifically, for level Vb, 13.3% (11/83) cases had LNs beyond the posteromedial border; for level VIIa, 1.5% (12/819) cases had LNs above the upper border, 5 (0.3%) cases had LNs located in the medial group. Moreover, we confirmed that no LN had been detected in certain areas of level Ib, II, IVa and Vc.

Potential modifications for neck CTV specific to NPC

According to LN distribution maps and distribution curves, neck node levels defined in 2013 updated consensus guidelines are comprehensive enough and boundaries described are applicable for most levels in most directions for NPC. However, by comparison of LN distribution and consensus guidelines, a new level VIIc was proposed to include medial group of retropharyngeal LNs. To draw CTV boundaries specific to NPC, moderate extended boundaries for levels Vb and VIIa were recommended, while it was suggested that reduced boundaries were possibly adaptable for levels Ib, II, IV and Vc. Nevertheless, all these modifications should be validated by prospective clinical trials. Fig.

4 illustrates the modifications.

1. Level VIIc: For retropharyngeal LN, consensus guidelines consider only the lateral group. In current study, 5 (0.3%) cases had LNs located in the medial group, which seems to be a part of neck lymphatic drainage network of NPC. None of the 5 LNs were below the caudal edge of second cervical vertebrae (C2). In order to better guide the elective irradiation of neck levels for NPC, we propose a new level VIIc to include the medial group of retropharyngeal LN. Proposed boundaries extend cranially from the skull base to the caudal edge of C2 vertebrae caudally. This space is bounded anteriorly by the pharyngeal constrictor muscles, posteriorly by the longus capitis, laterally by the medial boundary of level VIIa, and medially by the midline (Fig. 4A).

2. Level Vb: We confirmed that LNs emerged beyond the posteromedial border of level Vb in 13.3% cases with level Vb LNs, scattering around the transverse blood vessels superficially to the anterior edge of levator scapulae muscle. We recommend extending the posteromedial border of level Vb to the anterior edge of levator scapulae muscle to include the transverse blood vessels (Fig. 4B).

3. Level VIIa: As 12 cases with LNs exceeding the upper edge of the first cervical vertebrae (C1), we recommended the cranial border of level VIIa being extended from the upper edge of C1 vertebrae to the skull base (Fig. 4C).

4. Level Ib: LNs in level Ib were all scattered laterally and anteriorly to submandibular gland (SMG), and no LN was identified along the medial edge of SMG or within the gland parenchyma. As the presence of intraglandular LNs has been disputable (6) and in order to eliminate xerostomia after radiotherapy (7), we suggest that SMG might be spared when delineating the CTV of level Ib (Fig. 4D).

5. Level II: At C1 and C2 vertebrae levels, the sternocleidomastoid and splenius capitis muscles are

tightly integrated and we confirmed that no LNs were detected in the gap between them. Accordingly, the gap between sternocleidomastoid and splenius capitis muscle might be spared when delineating the CTV of level II at where they are tightly integrated (Fig. 4E).

6. Level IVa: We confirmed that no LNs were identified in the gap between sternocleidomastoid and infrahyoid ribbon muscles at level IVa. We suggest that anterior border of level IVa might be modified from anterior edge of sternocleidomastoid to the posterior edge of infrahyoid ribbon muscles (Fig. 4F).

7. Level Vc: We suggest that the anterior border of level Vc might be revised as omo-hyoid muscle to replace skin (Fig. 4G) as no LNs were identified in the gap between skin and omo-hyoid muscle.

Discussion

By marking 10651 LNs in 959 patients, we first established regional lymph node distribution probability maps and distribution curves for NPC. Neck node levels defined in 2013 updated consensus guidelines were proved to be comprehensive enough and boundaries described are applicable for most levels in most directions for NPC. Objective of this paper is to address neck node levels boundaries specific to NPC based on neck node distribution from a large patient cohort, rather than generate recommendations on elective irradiation of the node levels for NPC. In summary, we propose a new level VIIc to include medial group of retropharyngeal LN, recommend moderate extended boundaries for levels Vb and VIIa, and suggest that boundaries for levels Ib, II, IV and Vc might be reduced.

As all LNs were manually marked on a single template CT scan, accuracy of LN marking is closely related to the reliability of LN distribution, which determined our results. We regard the LN marking procedure considerably accurate for two reasons. Firstly, each LN was manually marked at the equivalent location of template CT scan with reference to adjacent anatomic landmarks based on pretreatment MR images by an experienced radiation oncologist and independently checked by another more experienced one; and we have always verified that the nodes marked at the specific location in the template CT were indeed those observed on the original planning CT. Secondly, although the patient's head was slightly hyper-extended in template CT than MR images due to the use of immobilization mask, patients were all supine and "neutral". As anatomic landmark adjacent to LNs were used, shifts of anatomical landmarks and the LNs were always consistent when position of patients slightly changed.

Generally, minimal axial diameter (MID) of 10 mm has been used as effective size criterion for metastatic LNs in clinical practice (8). Brekel et al. reported the diagnostic sensitivity of node

metastasis was only 41.7% per LN based on a MID of 10 mm; using 8 and 6 mm increased sensitivity to 54.2% and 69.4%, with specificity values of 96.8% and 91.9% respectively (9). Based on a MID of 10 mm, imaging underestimates 12 – 50% of LN micrometastases (10–12). Another study found 16% of LN defined on MR images with a MID of 4 – 9 mm were histologically metastatic, compared to only 0.6% with a MID < 4 mm (13). However, even with the use of modern imaging modalities, there is no reliable diagnostic tool available to detect microscopic neck node involvement in patients with clinically or radiologically negative nodes. Consequently, for more comprehensive consideration of potential risk areas to overcome the limitation of lacking pathological confirmation, we marked all nodes with a MID of ≥ 4 mm.

This is the first time that a very extensive neck node distribution probability maps were established for NPC, which visually demonstrate the distribution of neck nodes and can be used to guide the delineation of neck CTV boundaries, while previous studies were all based on image reading (14–18). Based on the distribution probability maps and distribution curves generated from LNs with a MID ≥ 4 mm, we proposed a new level VIIc to include the medial group of retropharyngeal LNs. Although only 5 (0.3%) cases had LN located in the medial group, it cannot be denied that medial retropharyngeal LN is a part of neck lymphatic drainage network of NPC. To minimize irradiation to constrictor muscles, proposed caudal boundary of level VIIc is set at the caudal edge of C2 vertebrae. However, the proposed boundaries need to be optimized in a larger patient cohort. Moreover, in which cases do level VIIc need prophylactic irradiation warrant further investigation.

From the results, we suggest to extend the posteromedial boundary of levels Vb and cranial boundary of level VIIa. For level Vb, we confirmed that, in 13.3% (11/83) cases, neck nodes beyond the posteromedial border of level Vb were indeed beyond that border, rather than resulted from the

differences in patient positioning (Figure E5). Similarly, insufficient posterior boundary was also found previously by reviewing MRI images from 3100 patients with NPC (14). Wang et al. suggested including the area between the levator scapulae and the anterior edge of the trapezius muscle as CTV, which is similar to our suggestion. For level VIIa, Wang et al. (15) assessed 597 retropharyngeal LNs in 392 patients, and found 37 (6.2%) were at the level of the occipital bone, beyond the cranial border of the body of C1. Liu et al. (16) showed 24 (9.6%) retropharyngeal LNs were located at the occipital level. These previously reported incidences seems to be higher than our results (12/819, 1.5%). Reasonable reason is that these studies assessed the entire volume of enlarged LNs, but our probability maps and distribution curves included only center point of the median slice of each LN to minimize the mass and distortion effects of enlarged nodes. Nevertheless, previous results can still support our modifications for level VIIa to some extent.

Due to impossibility of completely pathology examination of the lymphoid adipose tissue in NPC patients, our suggestions to reduce the boundaries of levels Ib, II, IVa and Vc should be treated with cautions as our LN distribution probability maps and distributions curves were simply image-concerned and whether they are consistence with truly neck lymphatic drainage is unknown. Accordingly, it is no doubt that our suggestions could not be adopted as routine clinical practice before there is an international consensus to reduce node levels boundaries. Nevertheless, all these suggestions were based on objective neck node distribution from 959 patients, which can provide foundation for further prospective studies and maybe revision of the guidelines.

For level Ib, it is commonly accepted that elective irradiation should be considered in certain circumstances, such as gross involvement of the ipsilateral SMG, oral cavity, anterior half of nasal cavity (17). After comprehensive analysis of 1084 level Ib LNs with a MID ≥ 4 mm from 959 patients,

we confirmed that no LN was identified along the medial edge of SMG or within the gland parenchyma. We therefore suggest that SMG might be spared when delineating CTV of level Ib. Previously, Poon et al. reported similar phenomenon in head and neck cancer, and suggested that beyond the scenario of oral tongue cancer, the SMG parenchyma do not need to be included in a typical elective nodal target volume (6). Moreover, xerostomia is the most common side effect of radiotherapy in NPC and preservation of SMG function is crucial to reduce xerostomia as SMG produces most of the unstimulated saliva (7). However, for NPC, safety of SMG sparing must be verified by prospective clinical trials.

For level II, LN distribution implicated that the gap between sternocleidomastoid and splenius capitis muscle might be spared when delineating the CTV of level II at where they are tightly integrated, this was similar to the recommendation by Zhang et al. (18). However, Zhang et al. (18) and Wang et al. (19) reported the cranial edge of level II did not fully cover all level II involvement, it was not verified by our study, probably as that we assessed only LN center point rather than total volume.

For levels IVa and Vc, although our study were simply image-concerned and no previous studies have focused on these two levels, reducing boundaries would have potential benefits for NPC patients. For level IVa, modifying the anterior border to the posterior edge of infrahyoid ribbon muscles could reduce doses to thyroid gland and might result in decreased incidence of long-term hypothyroidism (20, 21). At level Vc, the superficial skin is right the area of skin folds and prone to friction and breakage. If the anterior boundary of level Vc was modified from skin to omo-hyoid muscle, doses to skin could reduced and might eliminated radiation-induced dermatitis, which is one of the most common acute side effects of radiation and dose-dependent (22). Despite potential benefits, our suggestions warrant further confirmation in larger patient cohort and prospective studies.

Another issue need to be addressed is that we marked the center points of each LN on all emerge slices but used only center point of the median slice to establish distribution probability maps and distribution curves to minimize the mass and distortion effects of enlarged nodes. In future, we attempt to predict further LN metastasis probabilities of objective patients using this more comprehensive LN distribution information.

In conclusion, we established regional lymph node distribution probability maps and curves for NPC and confirmed that the majority of node levels in the 2013 updated consensus guidelines are comprehensive and applicable for NPC. While, we propose a new level VIIc to include medial group of retropharyngeal LNs, recommend moderate extended boundaries for levels Vb and VIIa, and suggested that boundaries for levels Ib, II, IV and Vc might be reduced.

References

1. Lee AW, Poon YF, Foo W, et al. Retrospective analysis of 5037 patients with nasopharyngeal carcinoma treated during 1976-1985: overall survival and patterns of failure. International journal of radiation oncology, biology, physics. 1992; 23(2):261-70.

2. Ho FC, Tham IW, Earnest A, Lee KM, Lu JJ. Patterns of regional lymph node metastasis of nasopharyngeal carcinoma: a meta-analysis of clinical evidence. BMC cancer. 2012;12:98.

3. Grégoire V, Levendag P, Ang KK, et al. CT-based delineation of lymph node levels and related CTVs in the node-negative neck: DAHANCA, EORTC, GORTEC, NCIC,RTOG consensus guidelines. Radiotherapy and Oncology. 2003; 69(3):227-36.

4. Gregoire V, Eisbruch A, Hamoir M, Levendag P. Proposal for the delineation of the nodal CTV in the node-positive and the post-operative neck. Radiotherapy and oncology: journal of the European Society for Therapeutic Radiology and Oncology. 2006; 79(1):15-20.

5. Gregoire V, Ang K, Budach W, et al. Delineation of the neck node levels for head and neck tumors: a 2013 update. DAHANCA, EORTC, HKNPCSG, NCIC CTG, NCRI, RTOG, TROG consensus guidelines. Radiotherapy and oncology. 2014; 110(1):172-81.

6. Poon I, Fischbein N, Lee N, et al. A population-based atlas and clinical target volume for the head-and-neck lymph nodes. International journal of radiation oncology, biology, physics. 2004; 59(5):1301-11.

7. Hawkins PG, Lee JY, Mao Y, et al. Sparing all salivary glands with IMRT for head and neck cancer: Longitudinal study of patient-reported xerostomia and head-and-neck quality of life. Radiother Oncol. 2017; doi: 10.1016/j.radonc.2017.08.002.

8. Tang L, Mao Y, Liu L, et al. The volume to be irradiated during selective neck irradiation in

nasopharyngeal carcinoma: analysis of the spread patterns in lymph nodes by magnetic resonance imaging. Cancer.2009; 115(3):680-8.

9. van den Brekel MW, Stel HV, Castelijns JA, et al. Cervical lymph node metastasis: assessment of radiologic criteria. Radiology.1990; 177(2):379-84.

10. Friedman M, Mafee MF, Pacella BL, Jr., Strorigl TL, Dew LL, Toriumi DM. Rationale for elective neck dissection in 1990. The Laryngoscope.1990; 100(1):54-9.

11. Righi PD, Kopecky KK, Caldemeyer KS, Ball VA, Weisberger EC, Radpour S. Comparison of ultrasound-fine needle aspiration and computed tomography in patients undergoing elective neck dissection. Head & neck.1997; 19(7):604-10.

12. van den Brekel MW, Castelijns JA, Stel HV, Golding RP, Meyer CJ, Snow GB. Modern imaging techniques and ultrasound-guided aspiration cytology for the assessment of neck node metastases: a prospective comparative study. European archives of oto-rhino-laryngology.1993; 250(1):11-7.

13. Vandecaveye V, De Keyzer F, Vander Poorten V, et al. Head and neck squamous cell carcinoma: value of diffusion-weighted MR imaging for nodal staging. Radiology.2009; 251(1):134-46.

14. Wang X, Hu C, Ying H, et al. Patterns of lymph node metastasis from nasopharyngeal carcinoma based on the 2013 updated consensus guidelines for neck node levels. Radiotherapy and oncology.2015; 115(1):41-5.

15. Wang XS, Hu CS, Ying HM, Zhou ZR, Ding JH, Feng Y. Patterns of retropharyngeal node metastasis in nasopharyngeal carcinoma. International journal of radiation oncology, biology, physics. 2009; 73(1):194-201.

16. Liu LZ, Zhang GY, Xie CM, Liu XW, Cui CY, Li L. Magnetic resonance imaging of retropharyngeal lymph node metastasis in nasopharyngeal carcinoma: patterns of spread. International

journal of radiation oncology, biology, physics. 2006; 66(3):721-30.

17. Zhang F, Cheng YK, Li WF, et al. Investigation of the feasibility of elective irradiation to neck level Ib using intensity-modulated radiotherapy for patients with nasopharyngeal carcinoma: a retrospective analysis. BMC Cancer. 2015;15:709.

18. Zhang J, Pan L, Ren J, et al. Level IIb CTV delineation based on cervical fascia anatomy in nasopharyngeal cancer. Radiotherapy and oncology. 2015; 115(1):46-9.

19. Wang X, Li L, Hu C, et al. Patterns of level II node metastasis in nasopharyngeal carcinoma. Radiotherapy and oncology. 2008; 89(1):28-32.

20. Lee V, Chan SY, Choi CW, et al. Dosimetric Predictors of Hypothyroidism After Radical Intensity-modulated Radiation Therapy for Non-metastatic Nasopharyngeal Carcinoma. Clinical oncology (Royal College of Radiologists (Great Britain)). 2016; 28(8):e52-60.

21. Wu YH, Wang HM, Chen HH, et al. Hypothyroidism after radiotherapy for nasopharyngeal cancer patients. International journal of radiation oncology, biology, physics. 2010; 76(4):1133-9.

22. Salvo N1, Barnes E, van Draanen J, et al. Prophylaxis and management of acute radiation-induced skin reactions: a systematic review of the literature. Curr Oncol. 2010 Aug;17(4):94-112.

Figure Legends

Figure 1. Visual examples of LN marking on the template CT scan.

(A) Axial T2-weighted MR images of a 35-year-old male showing five lymph nodes in bilateral level II; the left level IIa nodes are 7 × 10 mm and 6 × 6 mm (white arrows), the left level IIb node is 9 × 10 mm (blue arrow), the right level IIa node is 6 × 9 mm (yellow arrow), the right level IIb node is 14 × 15 mm (red arrow); (B) template CT scan at equivalent axial slice, 3mm circles represent the center points of emerge lymph nodes. Names of marked LNs consist of 3 parts connected using underscores, for example, in "788_$LN_{4\text{-}8mm}$_L1", 788 is patient number in the cohort, $LN_{4\text{-}8mm}$ means minimal axial diameter of this lymph node is 4 – 8mm, L1 means this is the first lymph node defined in left neck.

Figure 2. Distribution probability maps for the LNs demonstrated through five typical transverse sections.

(A1 – A5) $Map_{\geq 10mm}$, established based on LN_{RP} and $LN_{\geq 10mm}$; (B1 – B5) $Map_{\geq 8mm}$, based on LN_{RP} and $LN_{\geq 8mm}$ ($LN_{\geq 10mm}$ + $LN_{8\text{-}10mm}$); and (C1 – C5) $Map_{\geq 4mm}$, based on LN_{RP} and $LN_{\geq 4mm}$ ($LN_{\geq 10mm}$ + $LN_{8\text{-}10mm}$ + $LN_{4\text{-}8mm}$). The light blue lines denote neck node levels based on the 2013 updated consensus guidelines. Color wash changing from blue through yellow to red indicates probability increase.

Figure 3. Lymph node distribution curves and the 2013 updated consensus guidelines demonstrated through 8 transverse sections.

The light blue lines denote the neck node levels based on the latest international consensus guidelines. The red dotted lines denote $DC_{\geq 10mm}$, generated based on LN_{RP} and $LN_{\geq 10mm}$; the dark blue dotted lines denote $DC_{\geq 8mm}$, generated based on LN_{RP} and $LN_{\geq 8mm}$ ($LN_{\geq 10mm}$ + $LN_{8\text{-}10mm}$); and the yellow dotted

lines denote $DC_{\geq 4mm}$, generated based on the LN_{RP} and $LN_{\geq 4mm}$ ($LN_{\geq 10mm}$ + $LN_{8\text{-}10mm}$ + $LN_{4\text{-}8mm}$).

Figure 4. Illustrations of proposed new level VIIc and modifications of neck node levels boundaries for level VIIa, Vb, Ib, II, IVa and Vc.

Images on the left column show three distribution curves (red dotted lines, dark blue dotted lines and yellow dotted lines) along with the 2013 updated consensus guidelines (light blue lines). Images on the right column illustrate the modifications: (A) propose a new level VIIc to include medial group of retropharyngeal nodes; (B) extend the posteromedial border of level Vb to the anterior edge of levator scapulae muscle to include the transverse blood vessels; (C) extend the cranial border of level VIIa from the upper edge of C1 to the skull base; (D) submandibular gland being spared when delineating the CTV of level Ib; (E) gap between sternocleidomastoid and splenius capitis muscle being spared when delineating the CTV of level II at where they are tightly integrated; (F) anterior border of level IVa being modified from anterior edge of sternocleidomastoid to the posterior edge of infrahyoid ribbon muscles; (G) the anterior border of level Vc being revised as omo-hyoid muscle to replace skin.

Table 1. Characteristics of the 1000 patients with nasopharyngeal carcinoma

Characteristic	No. of patients (%)
Sex	
Male	751 (75.1)
Female	249 (24.9)
Age (years)	
Median	45 (18-78)
> 50	294 (29.4)
≤ 50	706 (70.6)
Histologic type	
Keratinizing squamous cell carcinoma	4 (0.4)
Non-keratinizing carcinoma	996 (99.6)
T stage[a]	
T1	120 (12.0)
T2	134 (13.4)
T3	524 (52.4)
T4	222 (22.2)
N stage[*]	
N0	142 (14.2)
N1	559 (55.9)
N2	166 (16.6)
N3	133 (13.3)
Clinical stage[*]	
I	35 (3.5)
II	149 (14.9)
III	494 (49.4)
IV	322 (32.2)

[*] Patients were re-staged according to the 8th edition of the AJCC (American Joint Committee on Cancer) / UICC (Union for International Cancer Control) staging system.

Table 2. Distribution of the 10651 lymph nodes in 959 patients

Level	Number (percentage) of patients			Number (percentage) of LNs		
	$LN_{\geqslant 10mm}$	$LN_{\geqslant 8mm}$	$LN_{\geqslant 4mm}$	$LN_{\geqslant 10mm}$	$LN_{\geqslant 8mm}$	$LN_{\geqslant 4mm}$
Ia	0	4 (0.4)	115 (12.0)	0	4 (0.08)	142 (1.3)
Ib	24 (2.5)	51 (5.3)	548 (57.1)	30 (0.7)	62 (1.3)	1084 (10.2)
II	587 (61.2)	686 (71.5)	949 (99.0)	1945 (45.1)	2311 (47.9)	5446 (51.1)
III	170 (17.7)	194 (20.2)	509 (53.1)	448 (10.4)	508 (10.6)	1411 (13.2)
IVa	49 (5.1)	57 (5.9)	161 (16.8)	98 (2.3)	110 (2.3)	311 (2.9)
IVb	4 (0.4)	5 (0.5)	10 (1.0)	6 (0.1)	7 (0.1)	13 (0.1)
Va	64 (6.7)	76 (8.0)	235 (24.5)	89 (2.1)	104 (2.2)	365 (3.4)
Vb	23 (2.4)	30 (3.1)	83 (8.7)	46 (1.1)	57 (1.2)	157 (1.5)
Vc	2 (0.2)	2 (0.2)	6 (0.6)	2 (0.05)	2 (0.04)	7 (0.07)
VIa	0	0	0	0	0	0
VIb	0	0	2 (0.2)	0	0	2 (0.02)
VIIa (LN_{RP})		819 (85.4)			1625 (15.3)	
VIIb	7 (0.7)	7 (0.7)	8 (0.8)	7 (0.2)	7 (0.1)	8 (0.08)
VIII	13 (1.4)	14 (1.5)	43 (4.5)	15 (0.3)	17 (0.4)	63 (0.6)
IX	1 (0.1)	1 (0.1)	2 (0.2)	1 (0.02)	1 (0.02)	2 (0.02)
Xa	1 (0.1)	1 (0.1)	1 (0.1)	1 (0.02)	1 (0.02)	1 (0.009)
Xb	3 (0.3)	4 (0.4)	11 (1.1)	3 (0.07)	4 (0.08)	11 (0.1)
Total	878 (91.6)	896 (93.4)	959 (100)	4316 (100)	4820 (100)	10648 (100)

Abbreviations: $LN_{\geqslant 10mm}$, cervical lymph nodes (LNs) meeting the diagnostic criteria for lymph node metastases; $LN_{\geqslant 8mm}$, cervical LNs with a minimal axial diameter (MID) ≥ 8 mm, or any size with central necrosis, a contrast-enhanced rim or extracapsular spread; $LN_{\geqslant 4mm}$, cervical LNs with a MID ≥ 4 mm, or any size with central necrosis, a contrast-enhanced rim or extracapsular spread. LN_{RP} = retropharyngeal lymph nodes, namely level VIIa.

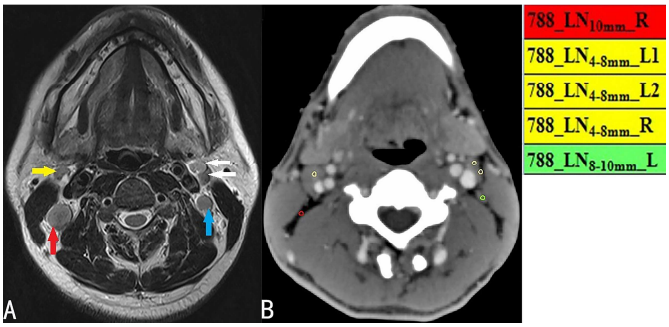

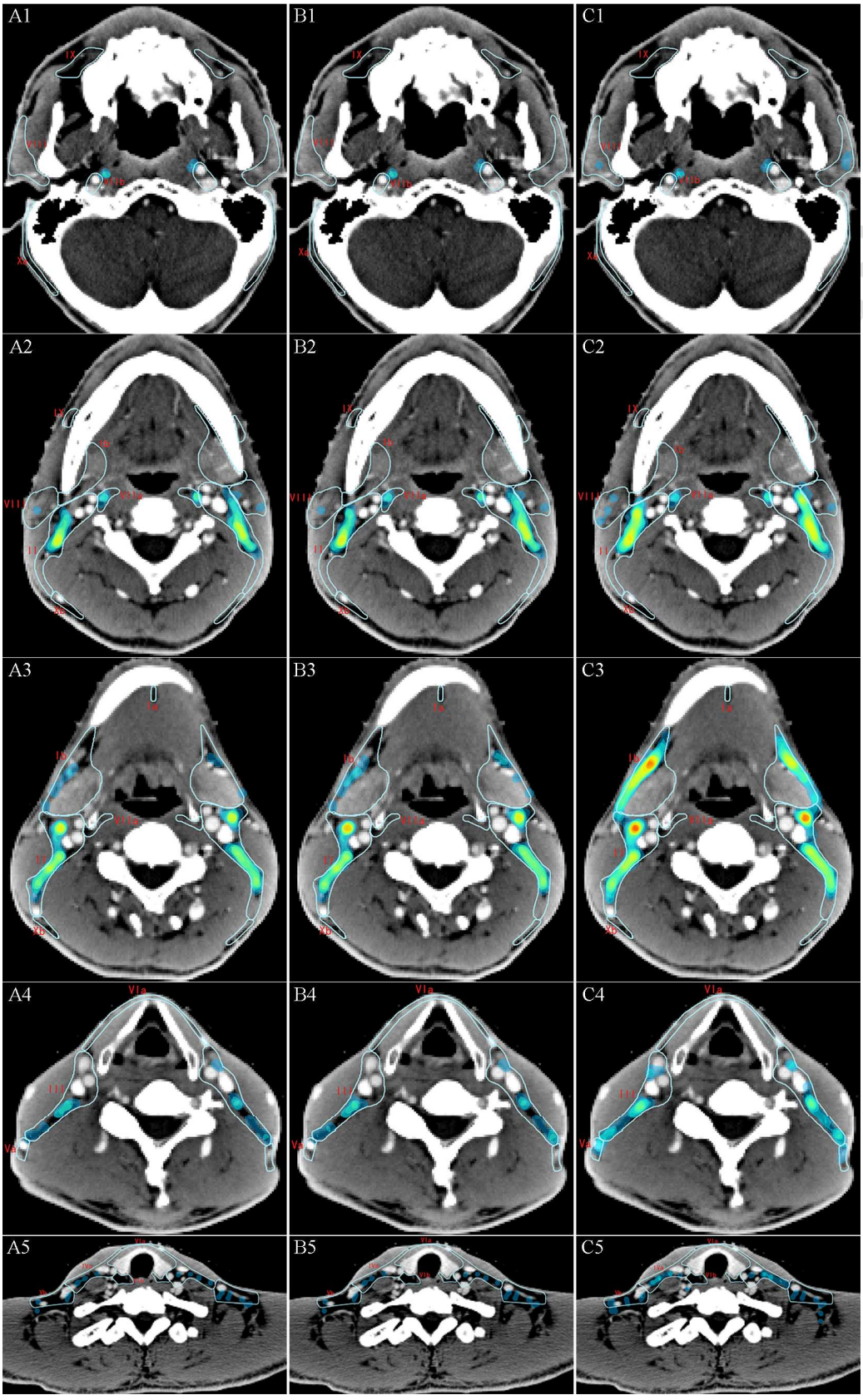
A1
B1
C1
A2
B2
C2
A3
B3
C3
A4
B4
C4
A5
B5
C5

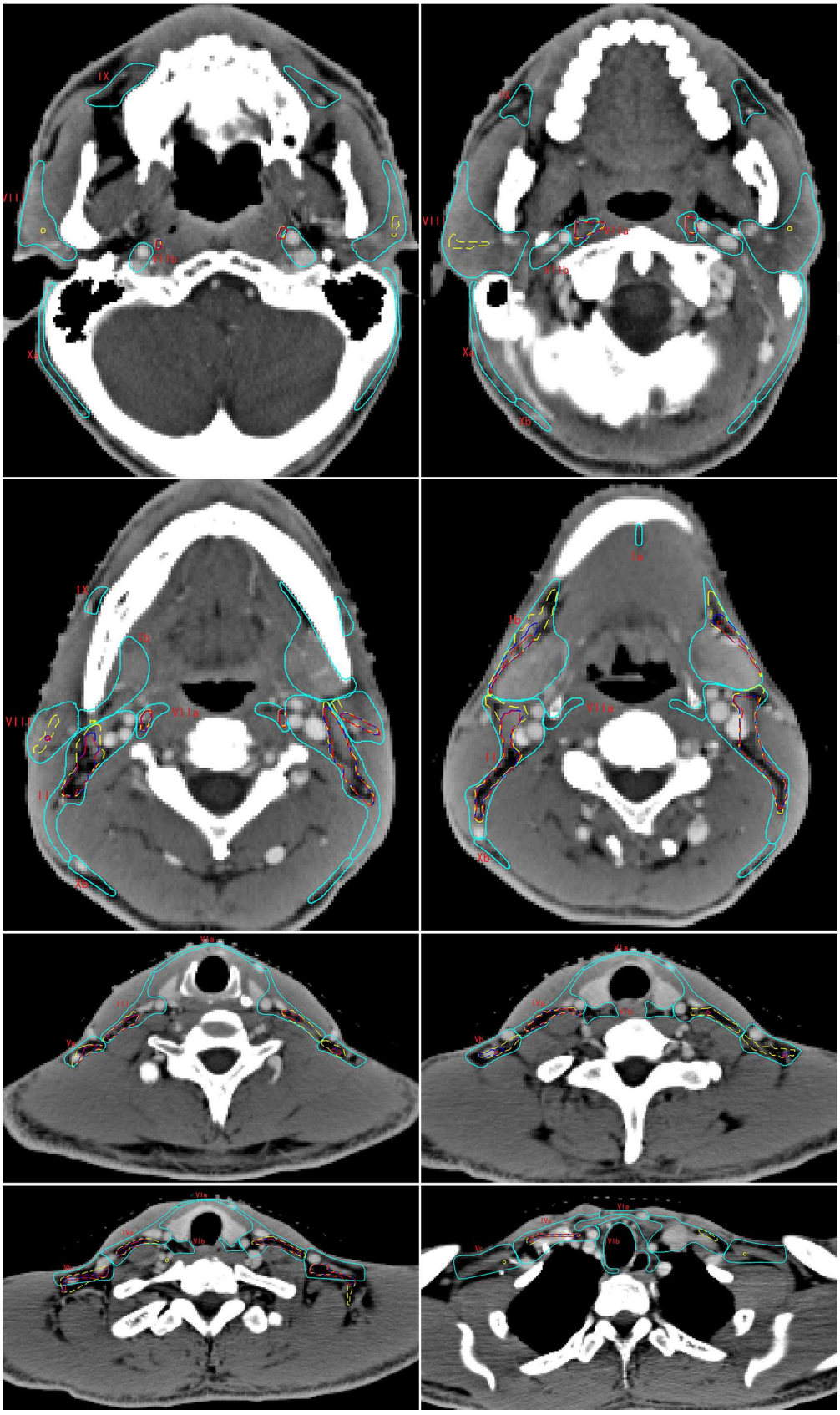
IX
VII
XI
Ia
Ib
II
III
IVa
Vb
VIa
VIb

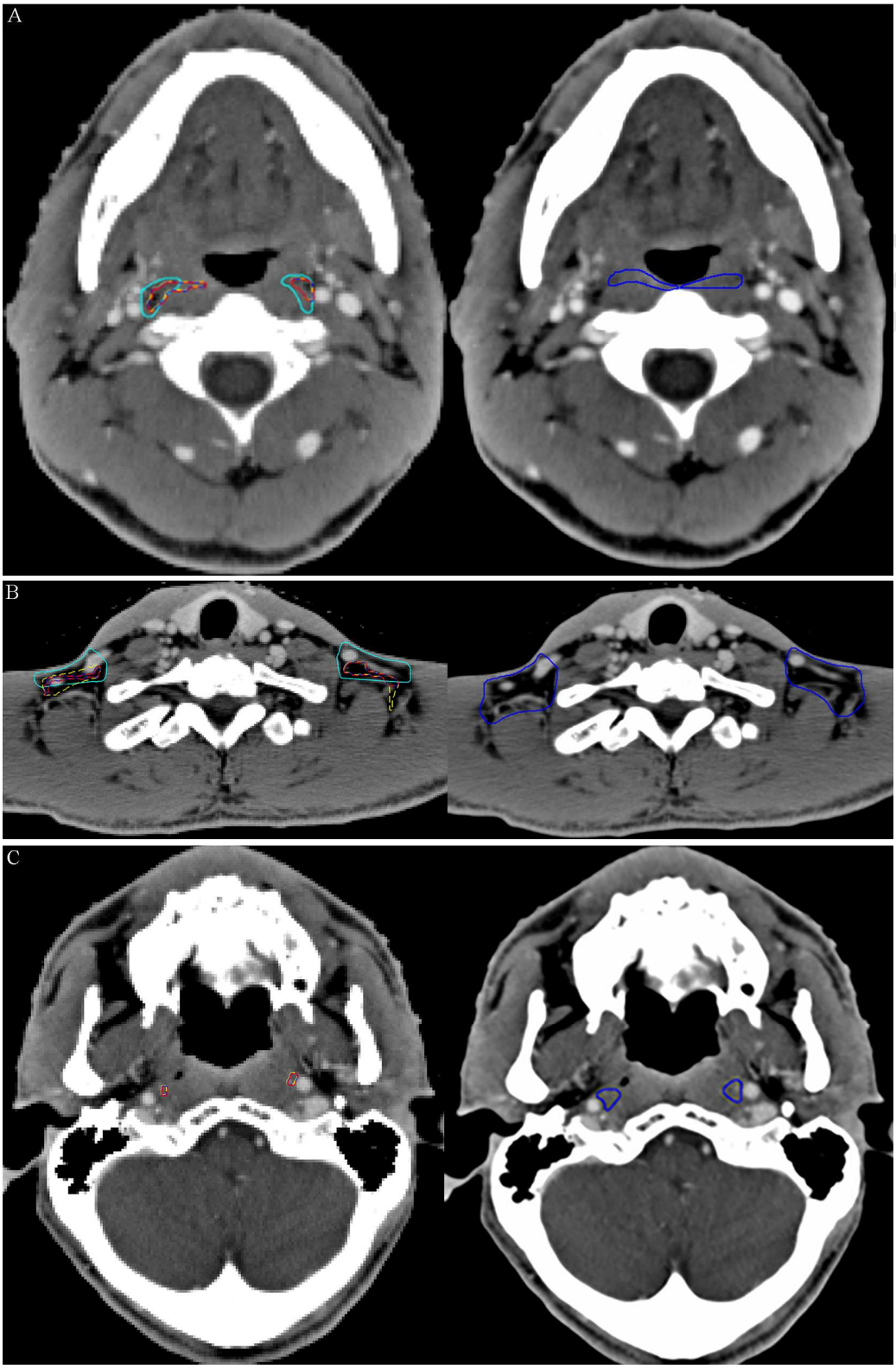
A
B
C

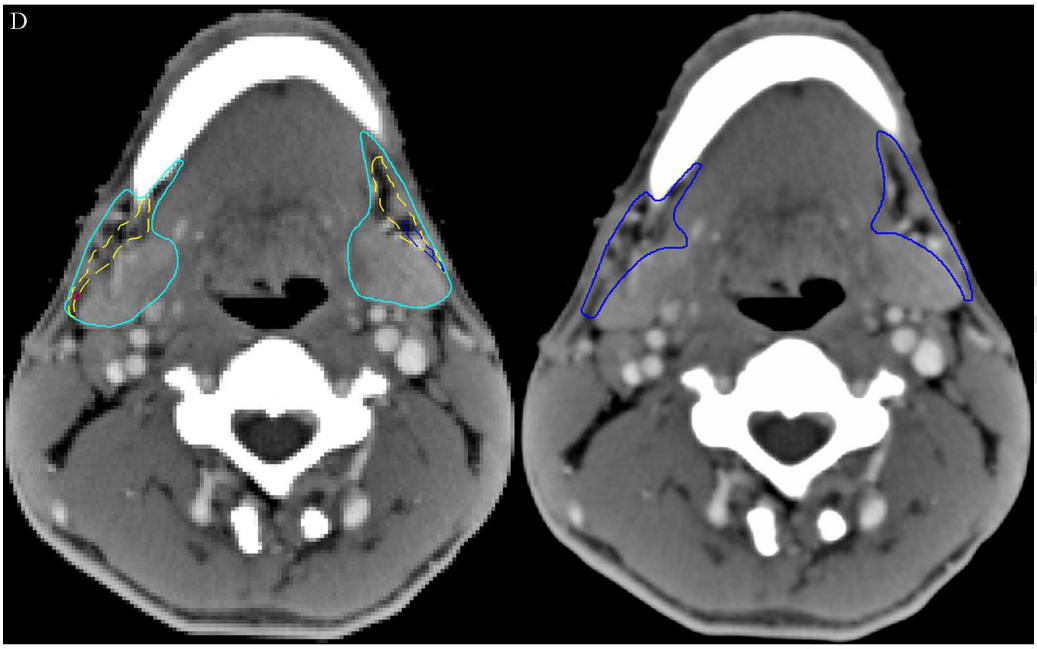
D

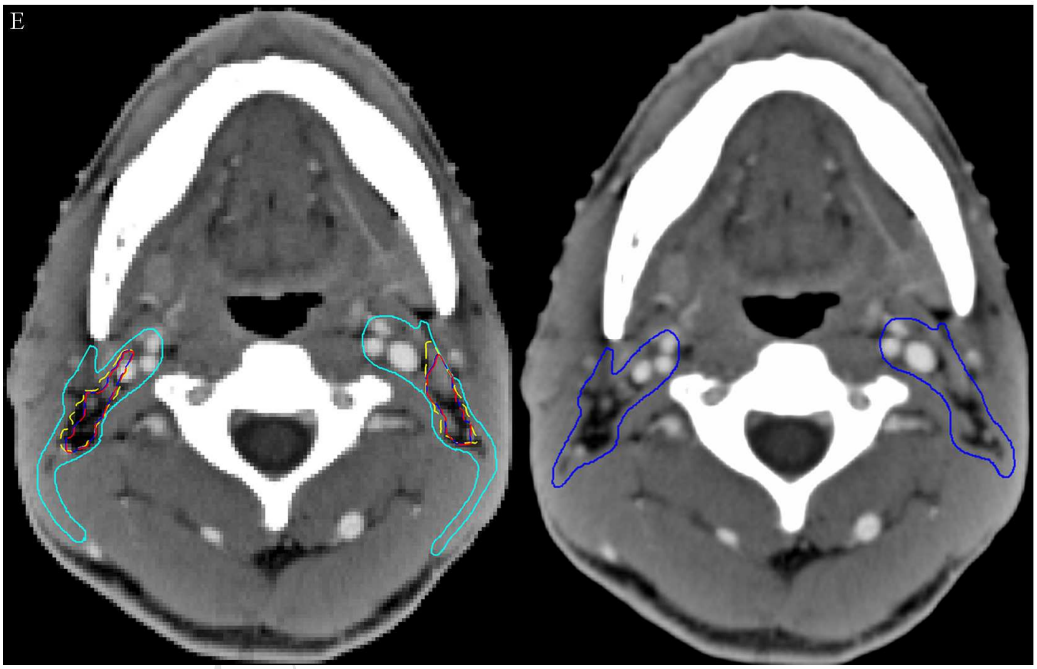
E

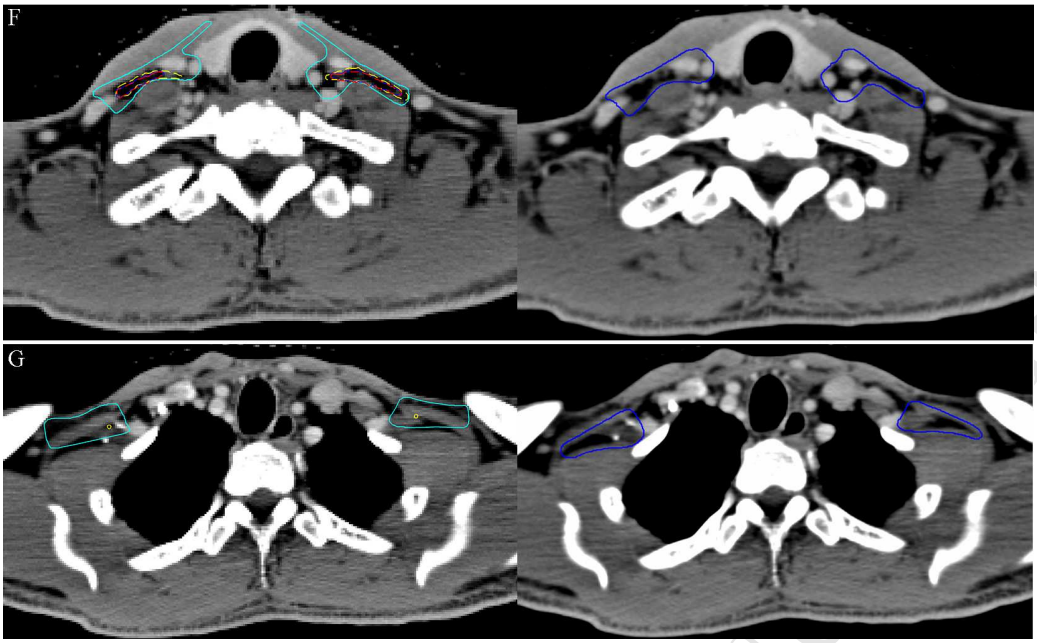

Summary

Neck node distribution probability maps and curves for NPC were established based on 10651 nodes from 956 patients. Relationships between node distribution and international consensus guidelines for delineation of neck node levels were analyzed. Our findings demonstrate that the majority of node levels in the 2013 updated consensus guidelines are comprehensive and applicable for NPC. We propose a new level VIIc to include medial group of retropharyngeal LNs, recommend moderate extended boundaries for levels Vb and VIIa, and suggest that boundaries for levels Ib, II, IV and Vc might be reduced.